7.10

A THEORY FOR THE PHASED-ARRAY WEATHER-RADAR TO MEASURE CROSSBEAM WIND, SHEAR AND TURBULENCE

Guifu Zhang[1*] and Richard J. Doviak[2]

1: School of Meteorology, University of Oklahoma, Norman, OK 73072
2: National Severe Storms Laboratory, Norman, OK 73072

ABSTRACT

The theory of measuring crossbeam wind, shear, and turbulence within the radar's resolution volume V_6 is described. Weather radar interferometry is formulated for such measurements using phased-array weather-radar. The formulation for a Spaced Antenna Interferometer (SAI) includes shear of the mean wind, allows turbulence to be anisotropic, and allows receiving beams to have elliptical cross sections. Auto- and cross-correlation functions are derived based on wave scattering by randomly distributed particles. Antenna separation, mean wind, shear, and turbulence all contribute to signal de-correlation. **C**rossbeam wind cannot be separated from shear and thus crossbeam wind measurements are biased by shear. It is shown that SAI measures an apparent crossbeam wind (i.e., the angular shear of the radial wind component). Whereas the apparent crossbeam wind and turbulence within V_6 cannot be separated using monostatic Doppler techniques, angular shear and turbulence can be separated using the SAI.

1. INTRODUCTION

Wind, shear and turbulence are important in quantifying and forecasting weather. Wind field is measured either by Doppler or interferometric techniques (Doviak and Zrnic, 2006; Doviak et al. 1996). Weather radars such as WSR-88Ds measure the Doppler velocity (i.e., the radial component of the scatterers' velocity) and its associated distribution (i.e., the spectrum width). But a Spaced Antenna Interferometer (SAI) such as NCAR's Multiple Antenna Profiler Radar (MAPR; Cohn et al. 2001) can, if wind is uniform, also measure the crossbeam wind, as well as the along-beam wind component within the radar's resolution volume V_6 The spaced antenna method was first applied to the measurement of crossbeam winds in the upper atmosphere (Briggs et al. 1950). Although assimilating multiple volume scans of radial velocity data in numerical models can retrieve wind field,; it is advantageous to have direct measurements of the crossbeam winds, and the SAI is one such instrument that can, under certain limitations discussed in this paper, provide such measurements.

However, applications of the SAI have been limited mainly to long wavelength (i.e., >6 m) radars for wind measurements in the Mesosphere-Stratosphere-Troposphere (MST) regions, and shorter wavelength (i.e., 30 cm) boundary layer profiling radars. The theory for these radars has been developed assuming anisotropic Bragg scatterers in uniform mean flow with isotropic turbulence Doviak et al. 1996). Recently, the SAI technique has received attention by the weather radar community. The MAPR was mounted on a pedestal to form a mechanically scanned beam. An X-band dual-polarization SA interferometer (DPSA; also with mechanically scanned beam) has been built and data has been collected with it for crossbeam wind measurement (Hardwick et al., 2005). Neither the scanning MAPR nor the DPSA has produced satisfactory crossbeam wind measurements due to various limitations, some of which are addressed herein. Turbulence and shear limit accurate measurement of crossbeam wind. Turbulence is usually calculated from spectrum width data, which can be corrupted by wind shear (Fang et al., 2004). The effect of shear on crossbeam wind measurement has not been fully understood and is addressed in this paper.

Another fundamental limitation is the requirement of a long dwell time at each beam direction for accurate crossbeam wind measurements using a SAI. This is contrary to the idea of fast scanning weather radar for large volume coverage. A phased-array weather-radar called the National Weather Radar Test Bed (NWRT) located at the National Severe Storms Laboratory in Norman, Oklahoma offers an opportunity to explore SAI techniques for crossbeam wind measurements using electronically scanned beams. The NWRT characteristics are described by Forsyth et al. (2005). The NWRT has pulse-to-pulse beam steering capability that provides better utilization of radar resources so that shorter dwell times for normal weather surveillance can be interlaced with longer ones for weather radar interferometry. Thus a NWRT type SAI can simultaneously survey weather and also measure crossbeam wind and shear, as well as turbulence along selected directions. A complete theory for such application has not been developed,.

We formulate the theory of weather radar interferometry for measurements of crossbeam wind, shear and turbulence for a SAI scanning precipitation. Auto- and cross-correlation functions are derived based on wave scattering by randomly distributed particles. The antenna separation, mean wind, shear and anisotropic turbulence are all taken into account in the formulation.

This paper is organized as follows: In Section 2 possible SAI configurations for the NWRT and their use is discussed. Weather radar interferometry is formulated

*: corresponding author: Guifu Zhang, School of Meteorology, University of Oklahoma, Norman, OK 73072, email: guzhang1@ou.edu

based on wave scattering from randomly distributed scatterers in Section 3; In Section 4 the composite of mean crossbeam wind and crossbeam shear of the mean longitudinal wind, the longitudinal wind, and turbulence are estimated from the auto and cross-correlation functions. The separation of turbulence from wind and shear measurements is discussed in this section.

2. POSSIBLE SAI CONFIGURATIONS FOR THE NWRT

The NWRT is the first phased-array weather-radar operating in the 10 cm wavelength band (the same as WSR-88Ds). The NWRT has been adapted from a monopulse antenna used for target detection and tracking. The antenna from an AN/SPY-1A radar (Brookner, 1988), and a transmitter from a WSR-88D weather radar are used for the NWRT. The NWRT transmits with all the array elements uniformly excited and receives signals with tapered weighting. The antenna has three ports (i.e., a sum, azimuth difference and elevation difference). Although the antenna's difference channels were disabled when it was transferred to the National Severe Storms Laboratory in Norman, Oklahoma, these channels are presently being activated.

One of the research/development objectives for the NWRT is to make instantaneous and direct measurement of wind components along and across the beam at each V_6 along the beam. The NWRT is capable of providing crossbeam wind and shear measurements within the beam while surveying the weather, a capability that does not exist with mechanically steered beams. The NWRT phased-array antenna allows SAI wind measurements without change to the antenna hardware. The sum and azimuth difference signals can be used to form an azimuth SAI with two virtual receivers, one for each of the left and right halves of the antenna as shown in Fig. 1a. Similarly, an elevation SAI can be constructed (Fig. 1b) from the sum and the elevation difference signals. A PAR in which one has access to many more elements would allow the receiving antennas to be overlapped so that better performance for wind measurements can be achieved in low signal-to-noise environments (Zhang et al. 2004).

The antenna patterns for the monopulse sum and difference channels are sketched in Fig. 2. Fig. 2a shows the full aperture beam as a circle, and the beam of the azimuth half aperture as an ellipse, corresponding to the azimuth SAI (Fig. 1a). The reduced azimuth resolution is due to the reduced antenna size in the azimuthal direction. Rotating the antenna patterns in Fig. 2a by 90 degrees leads to Fig. 2b, the beam cross sections for the zenith SAI (Fig. 1b). The elliptically shaped cross sections, of the receiving antennas' fields of view, are taken into account in the following formulation.

3. THEORY AND FORMULATION

Consider a SAI with the phase center of the transmitting aperture at T and that of two receiving antennas at R_1 and R_2, as shown in Fig. 3 of Zhang and Doviak (2007). Assume there is a spatial distribution of point scatterers, and that the *n*th scatterer is located at $\vec{r}_n(t)$ at time *t*. Distances from the scatterer to the transmitting and receiving antennas are $|\vec{r}_0-\vec{r}_n|$, $|\vec{r}_{01}-\vec{r}_n|$, and $|\vec{r}_{02}-\vec{r}_n|$ respectively. We have received signals at R_1 and R_2 expressed by

$$V(\vec{r}_{01},t_1)=\sum_{n=1}^{N}A_{1n}W_{1n}\exp\left[-jk\left(|\vec{r}_0-\vec{r}_n(t_1)|+|\vec{r}_{01}-\vec{r}_n(t_1)|\right)\right] \quad (1)$$

$$V(\vec{r}_{02},t_2)=\sum_{n=1}^{N}A_{2n}W_{2n}\exp\left[-jk\left(|\vec{r}_0-\vec{r}_n(t_2)|+|\vec{r}_{02}-\vec{r}_n(t_2)|\right)\right] \quad (2)$$

where A_{1n} is the prefilter echo-amplitude of the nth scatterer located at $\vec{r}_n(t_1)$ at time t_1, $\vec{r}_{01}$ is the vector distance from the center of V_6 to the receiver at R_1, and W_{1n} is a range dependent weight, a function of the transmitted pulse width and the receiver filter's bandwidth (Doviak and Zrnić, 2006, section 4.4). Similar definitions apply to (2). A_{1n} is proportional to the product of the square root of the power density patterns for the transmitting and receiving antennas. Because the range extent of V_6 is usually small compare to r_0 the small changes in the weighting function $W(r)$ due to the $1/r_0^2$ factor can be ignored.

Thus the cross-correlation of signals from the two receivers can be written as

$$C_{12}(t_2-t_1)=\langle V^*(\vec{r}_{01},t_1)V(\vec{r}_{02},t_2)\rangle=C_{12}(\tau) \quad (3)$$

under the assumption that signal statistics are stationary, where brackets indicate time or ensemble averaging, and t_2-$t_1\equiv\tau\equiv m$PRT $\equiv mT_s$ is the sample time spacing, and PRT = T_s is the Pulse Repetition Time. Therefore, substituting (1) and (2) into (3) and performing the integrations, we obtain

$$\begin{aligned}C_{12}(\tau)=&|A_0|^2 n(\vec{r}_0)g_T g_R 2^{1/2}\pi^{3/2}\sigma_R r_0^2\sigma_{e\theta}\sigma_{e\phi}\times\\ &\exp\left[-2jkv_{x'}(0)\tau-2k^2(\sigma_R^2 s_{x'}^2+\sigma_{tx'}^2)\tau^2\right]\times\\ &\exp\left[-k^2\sigma_{e\theta}^2\left(r_0 s_{z'}\tau+v_{z'}(0)\tau-\Delta z'_{12}/2\right)^2-k^2\sigma_{e\theta}^2\sigma_{tz'}^2\tau^2\right]\times\\ &\exp\left[-k^2\sigma_{e\phi}^2\left(r_0 s_{y'}\tau+v_{y'}(0)\tau-\Delta y'_{12}/2\right)^2-k^2\sigma_{e\phi}^2\sigma_{ty'}^2\tau^2\right]\end{aligned} \quad (4)$$

where $v_{x'}(0), v_{y'}(0)$, and $v_{z'}(0)$ are mean wind components and $s_{x'}, s_{y'}\ s_{z'}$ are wind shears. The effective one-way beamwidths in zenith and azimuth are defined by

$$\sigma_{e\theta}=\sqrt{\frac{2\sigma_{\theta T}^2\sigma_{\theta R}^2}{\sigma_{\theta T}^2+\sigma_{\theta R}^2}},\ \text{and}\ \sigma_{e\phi}=\sqrt{\frac{2\sigma_{\phi T}^2\sigma_{\phi R}^2}{\sigma_{\phi T}^2+\sigma_{\phi R}^2}} \quad (5)$$

respectively. Because the factors $\sigma_{e\theta},\sigma_{e\phi}$ in (5) are much smaller than 1 (for the NWRT $\sigma_{e\theta}\approx 10^{-2}$), the crossbeam components of turbulence typically contribute to signal de-correlation much less than the along-beam component.

On the other hand, if the beam is vertically, or nearly vertically, pointed, as it is always for wind profilers, and if turbulence is anisotropic (e.g., horizontally isotropic with significantly smaller vertical component), crossbeam turbulence could be relatively significant. But, if turbulence is isotropic, or nearly so, the contributions of crossbeam turbulence can be ignored as we henceforth assume.

If the receivers are matched and $\Delta z'_{12} = \Delta y'_{12} = 0$, $C_{12}(\tau) \to C_{11}(\tau) = C_{22}(\tau)$, the auto-covariances. At $\tau = 0$, the auto covariance equals the signal power *S*. Thus

$$C_{11}(0) \equiv S = |A_0|^2 \, n(\vec{r}_0) g_T g_R \sqrt{2}\pi^{3/2} \sigma_R r_0^2 \sigma_{e\theta} \sigma_{e\phi}, \qquad (6)$$

and the cross correlation coefficient is,

$$c_{12}(\tau) \equiv \frac{C_{12}(\tau)}{S} = \exp\Big[-2jkv_{x'}(0)\tau - 2k^2\left(\sigma_R^2 s_{x'}^2 + \sigma_{tx'}^2\right)\tau^2 - k^2\sigma_{e\theta}^2\left(\left(r_0 s_{z'} + v_{z'}(0)\right)\tau - \Delta z'_{12}/2\right)^2 - k^2\sigma_{e\phi}^2\left(\left(r_0 s_{y'} + v_{y'}(0)\right)\tau - \Delta y'_{12}/2\right)^2\Big] \qquad (7)$$

If there is no shear, it can be shown that (7) is exactly the same as the cross correlation of signals for Bragg scatter from refractive index perturbations (Doviak, et al., 1996; Eq.58) under the condition that the Bragg scatterers' correlation length transverse to the beam is small compared to the antenna diameter (i.e., Bragg scatter is isotropic). De-correlation of the signal by the mean wind advecting the scatterers out of V_6, is typically small and has been neglected.

Eq. (7) constitutes the theoretical formulation for SA weather radar interferometry in the presence of mean wind, turbulence, and shear. In using interferometry, we are primarily interested in the magnitudes of the auto- and cross-correlation functions, and henceforth we shall focus on the magnitude of (7). The second and third exponents account for signal de-correlation caused by longitudinal shear $s_{x'}$ and the longitudinal component $\sigma_{tx'}$ of turbulence. The remaining exponents account for signal de-correlation caused by the baseline shear, baseline wind, and receiving antenna separation. Baseline wind and shear are the crossbeam wind and shear parallel to a pair of SAI receivers. As seen from (7), baseline shear combines with baseline wind, and measurements of the correlation functions cannot separate the two.

Because weather radar beamwidths are small, it can be shown that factors $s_{z'} + v_{z'}(0)/r_0 \equiv s_\theta$ and $s_{y'} + v_{y'}(0)/r_0 \equiv s_\phi$ are approximately angular shears, of the mean radial wind. Angular shears are defined as the radial velocity change per differential arc length (e.g., $r_0 \sin\theta_0 d\phi$). Thus, $s_\phi = \dfrac{1}{r_0 \sin\theta_0}\dfrac{\partial v_r}{\partial \phi}$ is the azimuthal angular shear of the radial wind component v_r. Angular shears can also be determined from Doppler measurements at two or more angles in each direction; this measurement is called Doppler Beam Swinging (DBS; a variant of the Velocity Azimuth Display –VAD-technique commonly used to determine vector winds from weather observations with a single Doppler radar). Either the DBS or SAI method can be used to estimate the angular shear of the radial velocity. But, given the same resolution, and a high signal to noise ratio, the SAI method provides a more accurate measure than the DBS method. The DBS method is employed by wind profilers to measure wind, typically under the assumptions that wind is uniform over the region scanned by the beams, and that shear of the vertical wind can be ignored. Ignoring horizontal shear of the vertical wind should be a reasonable assumption for fair weather conditions, but under disturbed conditions this shear could cause significant errors in wind measurements. The effects of shear on wind measurements with profilers was evident in experiments in which six measuring systems were compared; on days of relatively unperturbed flow, estimated winds agreed very well, but the agreement was sporadic on days in which the convective boundary layer was active.

As stated above, cross correlation measurements of weather signals cannot distinguish baseline shear from baseline wind. Thus shear biases measurements of crossbeam wind within V_6 .Eq. (7) has also been verified with numerical simulations of wave scattering by a layer of randomly distributed particles moving across the beam. Cross-correlation functions are estimated from the simulated time-series data. Indeed, the baseline shear of along-beam wind causes the cross-correlation peak to move toward positive or negative time lags depending on whether shear is positive or negative.

Figure 3 shows the cross-correlation coefficient as a function of τ. The parameters of the NWRT were used for the calculation. Both auto- and cross-correlation coefficients at various ranges are shown in Fig. 3a. At near ranges, signal de-correlation is mainly caused by the antenna separation, crossbeam wind, and turbulence. Previous studies that ignored shear showed turbulence plays a significant role in de-correlating signals because its effect on the correlation time, compared to that caused by baseline wind, is multiplied by the ratio of the transmitting antenna diameter to. But shear is also a significant factor in de-correlating the signals, especially at long ranges where beamwidths are large. Because σ_R is independent of range, and turbulence is assumed to be uniform, the change in correlation time with range is only due to crossbeam shear.

Fig. 3b shows the correlation coefficients for weather signals from scatterers at a fixed range of 30 km, and for various shears along the baseline. Increases of baseline shear not only decrease the correlation time, but it also shifts the time lag to the peak of the cross correlation function.

Examination of (7) also shows that longitudinal shear $s_{x'}$ combines with turbulence $\sigma_{tx'}$ and thus turbulence measurements are biased by $s_{x'}$. Because range resolution is fine, longitudinal shear is typically small compared to turbulence and can be neglected. If it is not, methods must be found to separate the two. For example, the longitudinal shear bias to turbulence can be diminished by decreasing σ_R, Therefore longitudinal shear $s_{x'}$ can be determined by using different range resolutions. But baseline shear bias to baseline wind cannot be diminished by decreasing beamwidth.

Although there appears to be no practical method to separate baseline shear from baseline wind, measurement of the apparent baseline wind (e.g., $v_{ay'}(0) = r_0 s_{y'} + v_{y'}(0)$), obtained simultaneously everywhere along the beam, might provide useful constraints to sophisticated retrieval algorithms that can generate the fields of vector winds over large domains. Henceforth further discussion is focused on measurements of the apparent baseline wind and turbulence. We need to distinguish a definition of apparent wind used in early observations with SAIs. That apparent wind is baseline wind biased by turbulence and/or cross baseline wind, whereas the apparent wind defined herein is baseline wind biased by baseline shear. This apparent baseline wind can also be treated as the angular shear of the radial wind $s_\phi = s_{y'} + v_{y'}(0)/r_0$.

4. ESTIMATION OF THE APPARENT BASELINE WIND AND TURBULENCE

4.1 Estimation of wind

We can calculate the apparent baseline winds from the cross-correlation function using a cross-correlation ratio (CCR) method or the Full Correlation Analysis (FCA) method. For example, the apparent azimuth baseline wind component (i.e., $v_{ay'}(0)$) can be calculated from the cross-correlation function for signals from SAI's azimuth receivers (Fig. 1b) for which $\Delta z'_{12}$ = 0 in (7). The logarithm of the cross-correlation magnitudes at equal positive and negative lags leads to

$$L_\phi(\tau) = \ln \frac{\left|c_{12}^{(\phi)}(\tau)\right|}{\left|c_{12}^{(\phi)}(-\tau)\right|} = 2k^2 \sigma_{e\phi}^2 \Delta y'_{12} v_{ay'}(0)\tau \,. \qquad (8)$$

Thus, the apparent baseline wind $v_{ay'}(0)$ is given by:

$$v_{ay'}(0) = \frac{L_\phi(\tau)}{2k^2 \sigma_{e\phi}^2 \Delta y'_{12} \tau} \,. \qquad (9)$$

In a similar way, if two SAI receiving antennas are separated in the zenith direction, the apparent baseline wind component $v_{az'}(0)$ can be calculated. Hence, angular shears s_θ and s_ϕ within V_6 are obtained.

Because baseline shear combines with baseline wind, the accuracies of measuring the apparent baseline wind (or angular shear) can be directly derived from theoretical error analysis developed for baseline wind measurements in absence of shear (e.g., Zhang et al., 2004). It is shown that standard deviation of the apparent baseline wind estimates increase with range is due to the increased effect of the vertical shear. Compared to measurements of the along-beam wind component using Doppler measurements, baseline wind measurement requires longer dwell times. For example, if the turbulence $\sigma_{tx'} = 0.5$ m s^{-1}, about 5 seconds of data collection time is required to achieve an azimuthal apparent baseline wind, $v_{ay'}(0)$, measurement accuracy of 2.0 $m\ s^{-1}$ using the NWRT at near ranges. On the other hand, Doppler velocity (i.e., the radial wind component) can be measured with accuracies better than 1 m s^{-1} in a collection time two orders of magnitude shorter. The crossbeam wind estimated using DBS is degraded by a factor of $1/\Delta\theta$ in which $\Delta\theta$ is the angular separation, leading to poor measurement.

4.2 Estimation of turbulence; comparison with the dual-beamwidth method

Turbulence can estimated from spectrum width (or equivalently the correlation time of the auto-correlation function) using single-beamwidth (1BW) Doppler weather radars such as WSR-88D. Such estimation is neither accurate nor reliable because beam broadening and shear (Doviak and Zrnic, 2006; section 5.3) bias the turbulence estimates. It has been shown that layers of unusually large spectrum widths (e.g., larger than 8 m s^{-1}), suggestive of turbulence hazardous to safe flight, are seen in stratiform precipitation. But these large widths are principally due to shear, and are not necessarily hazardous to safe flight. It is difficult to separate the shear and turbulence contributions to spectrum width, especially if strong shear is confined to layers thin compared to V_6. Thus finding an accurate way to estimate turbulence could be advantageous. With the SAI method, turbulence can be directly calculated from (7). Comparisons of turbulence measurements using the SAI method and ones obtained using a beam sufficiently narrow that transverse shear of radial wind can be ignored showed good agreement, confirming the robustness of the SAI method for the measurement of turbulence.

Recently, a dual-beamwidth (2BW) radar method was applied to the MU VHF profiling radar to measure turbulence using the DBS method (VanZandt et al. 2002). The dual beam method separates the effect that vertical shear of horizontal wind has on turbulence measurements when off vertical-beams are used. Off-vertical beams are required at long wavelengths because vertical incidence backscatter, from Bragg scatterers having a correlation length not significantly smaller than the antenna diameter, introduces an unknown multiplicative factor that combines with turbulence σ_t. The use of an off-vertical beam mitigates the backscatter from Bragg scatterers of unknown correlation lengths. Here, we propose to extend the dual-beam method to an anisotropic beam pattern to estimate shear and turbulence. Dual-beam width signals are indeed obtained from the NWRT/SAI (i.e., the sum channel gives a narrow-beam signal and each half of the receiving aperture gives broad-beam signals).

By letting $\Delta y'_{12} = \Delta z'_{12} = 0$ in (7), we have the auto-correlation function magnitude

$$|C_N(\tau)| \approx S_N \exp\left[-2k^2\sigma_{tx'}^2\tau^2 - k^2 r_0^2 \sigma_{e\theta N}^2 (s_\theta \tau)^2 - k^2 r_0^2 \sigma_{e\phi N}^2 (s_\phi \tau)^2\right] \quad (10)$$

for the narrow-beam, and

$$|C_B(\tau)| \approx S_B \exp\left[-2k^2\sigma_{tx'}^2\tau^2 - k^2 r_0^2 \sigma_{e\theta B}^2 (s_\theta \tau)^2 - k^2 r_0^2 \sigma_{e\phi B}^2 (s_\phi \tau)^2\right] \quad (11)$$

for the broad-beam.

Using azimuth dual-beams, we have $\sigma_{e\theta 1} = \sigma_{e\theta 2} = \sigma_{e\theta} = \sigma_{\theta T}$, $\sigma_{e\phi 1} = \sigma_{\phi T}$, and $\sigma_{e\phi 2} = \sqrt{8/5}\sigma_{\phi T} \approx 1.26\sigma_{\phi T}$. Taking a ratio of the normalized auto-correlation magnitudes, and then taking the logarithm of the ratio, we obtain

$$\ln\frac{|C_N(\tau)||C_B(0)|}{|C_B(\tau)||C_N(0)|} = k^2 r_0^2 (\sigma_{e\phi B}^2 - \sigma_{e\phi N}^2)(s_\phi \tau)^2 . \quad (12)$$

Solving s_ϕ from Eq. (12), we obtain azimuthal shear s_ϕ, as represented by the dual-beam auto-correlations

$$s_\phi^2 = \frac{1}{k^2 r_0^2 (\sigma_{e\phi B}^2 - \sigma_{e\phi N}^2)\tau^2} L_S(\tau) \quad (13)$$

where

$$L_S(\tau) = \ln\frac{|C_B(0)|}{|C_B(\tau)|} - \ln\frac{|C_N(0)|}{|C_N(\tau)|} . \quad (14)$$

In the same procedure as above, elevation shear s_θ can be obtained. When s_θ and s_ϕ are known, they are substituted into (10) or (11) for one of the beam, to obtain turbulence $\sigma_{tx'}$. In the case that azimuthal shear s_ϕ is negligible, we can estimate turbulence using the elevation dual-beam auto-correlation ratio

$$\sigma_{tx'}^2 \approx \frac{1}{2k^2 r_0^2 (\sigma_{e\theta B}^2 - \sigma_{e\theta N}^2)\tau^2} L_T(\tau) \quad (15)$$

with

$$L_T(\tau) = \sigma_{e\theta B}^2 \ln\frac{|C_N(0)|}{|C_N(\tau)|} - \sigma_{e\theta N}^2 \ln\frac{|C_B(0)|}{|C_B(\tau)|} \quad (16)$$

Eqs. (13) and (15) combined with (14) and (16) are the same as the Eqs. (3) and (4) of VanZandt et al. (2002) except that two beam auto-correlation functions and correlation times are used instead of the spectrum widths used in VanZandt's expressions. These dual-beam derived shear and turbulence can be compared with those estimated using SA interferometry with a single radar system in NWRT.

5. SUMMARY AND CONCLUSIONS

We developed a theory for weather radar interferometry to measure, with a Spaced Antenna Interferometer (SAI), crossbeam wind, turbulence and shear within the radar's resolution volume V_6. Although the SAI has principally been applied to measurements of the cloud-free atmosphere, it has potential application to future weather radars. We formulate the problem based on scattering from randomly distributed particles, allow the receiving beams to have elliptical cross sections (required if full receiving apertures are used), and consider anisotropic turbulence and shear, whereas previous formulations assumed Bragg scatter, circular beams, uniform wind, and isotropic turbulence. Cross- and auto-correlation functions, of the weather signals received by a pair of SAI receivers, are derived. If turbulence is isotropic the theory shows that turbulence transverse to the beam contributes negligibly to the correlation functions.

It is shown that mean baseline wind (i.e., the crossbeam wind parallel to the baseline connecting a pair of SAI receivers) within V_6 cannot be separated from baseline shear of the mean longitudinal (i.e., along the beam) wind. That is, baseline wind and shear combine to form an angular shear of the radial velocity. Nevertheless, the SAI can separate turbulence from shear, whereas this separation cannot be made using Doppler techniques. SAI turbulence measurements could improve quantification of atmospheric turbulent kinetic energy and measurements of turbulence within V_6.

It is suggested that SAI simultaneous measurements of the angular shear along the beam at chosen beam directions could provide additional observational constraints on the numerically derived wind field. Efforts are now underway to upgrade the NWRT to allow SAI measurements so that crossbeam wind and/or shear can be measured along with radial velocities. It has been shown that accurate measurement of crossbeam is difficult to achieved even with SAI, especially at farther ranges. SAI, however, provides another way to separate shear from turbulence, and accurate turbulence measurement.

Acknowledgements

The authors greatly appreciate helpful discussions with Drs. D. S. Zrnić, Q. Xu and D. Forsyth of the National Severe Storms Laboratory, and Drs. M. Xue, R. Palmer and H. Bluestein of the University of Oklahoma. Many thanks go to Lockheed Martin and NSSL's engineers for developing the NWRT. This work was partially supported by NOAA/NSSL under the cooperative agreement NA17RJ1227.

6. References

Briggs, B. H., G. J. Phillips, and D. H. Shinn, 1950: The analysis of observations on spaced receivers of the

fading radio signals, *Proc. Phys. Soc. London Sec. B,* **63**, 106-121.
Brookner, E, *Aspects of Modern Radar*. Artech House, 1988, 574 pp.
Cohn, S. A., W. O. J. Brown, C. L. Martin, M. S. Susedik, G. Maclean, and D. B. Parsons, 2001: Clear Air Boundary Layer Spaced Antenna Wind Measurement with the Multiple Antenna Profiler (MAPR), *Annales Geophysicae*, **19**(8), 845-854.
Doviak, R. J., and D. S. Zrnic, 2006: *Doppler radar and weather observations*. Dover Publishers, Mineola, N.Y. 1150pp.
Doviak, R. J., R. J. Lataitis, and C. L. Holloway, 1996: Cross correlation and cross spectra for spaced antenna wind profilers: 1. Theoretical analysis. *Radio Sci.* **31**, 157-180.
Fang, M., R. J. Doviak, and V. Melnikov, 2004: Spectrum Width Measured by WSR-88D: Error Sources and Statistics of Various Weather Phenomena. *J. Atmos. Oceanic Technol.*, **21**, 888–904.
Forsyth, D., J. Kimpel, D. Zrnic, R. Ferek, J. Heimmer, T. McNellis, J. Crain, A. Shapiro, R. Vogt, and W. Benner, 2005: The National Weather Radar Testbed (Phased-Array). in 32nd Conference on Radar Meteorology, 24-29 October, Albuquerque, NM., Amer. Meteor. Soc.,12R.3.
Hardwick, K. M., S. J. Frazier, A. L. Pazmany, 2005: Spaced antenna measurements of cross beam velocity in severe storms. *32nd Int. Conf. on Radar Meteorology*, Albuquerque, NM., Amer. Meteor. Soc, P4R.11.
VanZandt, T. E., G. D. Nastrom, J. Furumoto, T. Tsuda, and W. L. Clark, 2002: A dual-beamwidth radar method for measuring atmospheric turbulent kinetic energy, *Geophy. Res. Let.,* **29**, no. 12, 10.1029/2001GL014283.
Zhang, G., R. J. Doviak, J. Vivekanandan, W. Brown, and S. A. Cohn, 2004: Performance of correlation estimators for spaced antenna wind measurement in the presence of noise, *Radio Sci.* **39**, RS3017, doi:10.29/2003RS003022.
Zhang, G., and R. J. Doviak, J. Vivekanandan, 2007: Weather radar interferometry to measure crossbeam wind, shear and turbulence, To appear in *J. Atmos. Ocean. Tech.*

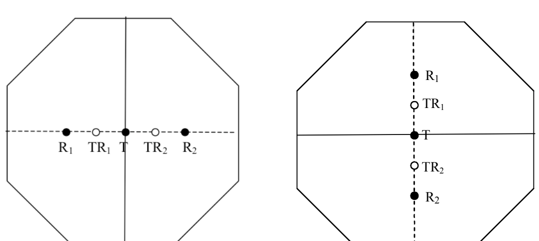

(a) (b)
Figure 1: The NWRT antenna configuration of receiving apertures R_1, R_2 for SA weather radar interferometry for (a) azimuth SAI, and (b) elevation SAI.

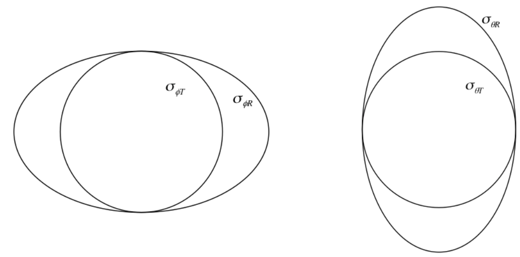
(a) (b)
Figure 2: Sketch of transmitting and receiving antenna beamwidths for the NWRT. The inner circles represents the transmitting beam (also the beam associated with the receiving sum channel), and the outer ellipse is the beam associated with one of the SAI receiving apertures. (a): azimuth SAI, and (b) zenith SAI. The theoretical transmitting and receiving beamwidths are: $\theta_{1T} = 2.36\sigma_{\theta T} \approx 1.53°$, and $\theta_{1R} = 2.36\sigma_{\theta R} \approx 3.06°$.

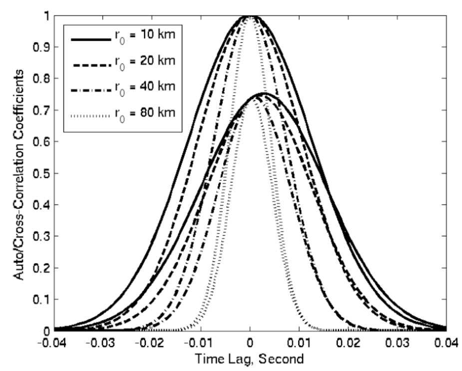

(a)

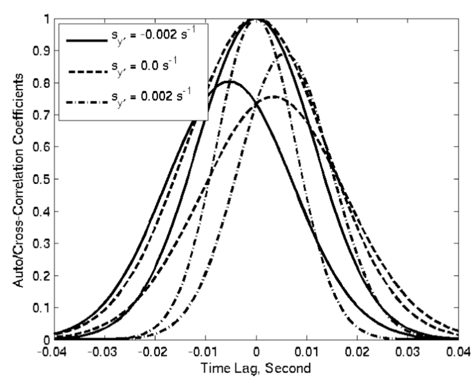

(b)
Figure 3. Auto- and cross-correlation coefficients vs τ at r_0 =10, 20, 40, and 80 km for NWRT parameters: λ = 0.0938 m, $\Delta y'_{12}$ = 1.46 m, $\Delta z'_{12}$ = 0.0 m, $\sigma_{\phi T}$ = 0.65°, $\sigma_{\phi R}$ = 1.30°. Meteorological parameters are: $v_{y'}(0)$ = 20, $v_{z'}(0)$ = 5, $\sigma_{tx'} = \sigma_{ty'} = \sigma_{tz'} = 0.5$ m s^{-1}, $s_{x'} = 0$. (a) Dependence on r_0; $s_{y'} = 0.0$, $s_{z'} = 0.002$ s^{-1}; (b) Dependence on shear $s_{y'}$ at r_0 = 30 km; $s_{z'} = 0.0$.